DNA Bending by the Mammalian High Mobility Group Protein AT Hook 2

Bo Chen, **Jasmine Young**, and **Fenfei Leng**[*]

Department of Chemistry & Biochemistry, Florida International University, 11200 SW 8th Street, Miami, FL 33199

Abstract

The mammalian high mobility group protein AT hook 2 (HMGA2) is a DNA binding protein that specifically recognizes the minor groove of AT-rich DNA sequences. Disruption of its expression pattern is directly linked to oncogenesis and obesity. In this paper, we constructed a new plasmid pBendAT to study HMGA2-induced DNA bending. pBendAT carries a 230 bp DNA segment containing 5 pairs of restriction enzyme sites, which can be used to produce a set of DNA fragments of identical length to study protein-induced DNA bending. The DNA fragments of identical length can also be generated using PCR amplification. Since pBendAT does not contain more than 3 consecutive AT base pairs, it is suitable for the determination of DNA bending induced by proteins recognizing AT-rich DNA sequences. Indeed, using pBendAT, we demonstrated that HMGA2 is a DNA bending protein and bends all three tested DNA binding sequences of HMGA2, SELEX1, SELEX2, and PRDII. The DNA bending angles were estimated to be 34.2, 33.5, and 35.4°, respectively.

Keywords

HMGA2; AT hook; DNA bending

The mammalian high mobility group protein AT-hook 2 (HMGA2) is a transcriptional factor involved in mesenchymal cell differentiation and transformation (1-3). It plays an important role in fat cell proliferation (2) and is considered to be a potential target for treatment of obesity (2,4). HMGA2 is also an onco-protein associated with the formation of a variety of tumors including benign tumors, such as uterine leiomyomas (5), lipomas (6,7) and pulmonary chondroid hamartomas (8), and malignant tumors, such as lung cancers (9-11), breast cancers (12), and leukemia (13). Interestingly, the expression level of HMGA2 was demonstrated to be correlated with the degree of malignancy, the existence of metastasis, and a poor prognosis for certain cancers (14,15). These results suggest that HMGA2 is a potential target for treatment of these cancers (4,16,17).

HMGA2 is a DNA binding protein containing three "AT hook" DNA binding domains that specifically recognize the minor groove of AT rich DNA sequences (18). Although each "AT hook" DNA binding domain binds to five AT base pairs (18,19), the high-affinity binding of HMGA2 requires two to three appropriated spaced 5-bp AT-rich DNA sequences as a single

[*] To whom correspondence should be addressed: Department of Chemistry & Biochemistry, Florida International University, 11200 SW 8th Street, FL 33199. Tel: 305-348-3277; Fax: 305-348-3772; lengf@fiu.edu.

multivalent binding site (20). The DNA binding constant of the multivalent binding is much greater than that of the single valent binding (21). Previously, using a PCR-based systematic evolution of ligands by exponential enrichment (SELEX) procedure, we identified two consensus sequences for HMGA2: 5′-ATATTCGCGAWWATT-3′ or 5′-ATATTGCGCAWWATT-3′ where W = A or T (21). Our results showed that the three segments in the consensus sequences (two AT-rich segments and one GC-rich segment) are required for high affinity binding; mutations of these sequences significantly reduced the DNA-binding affinity of HMGA2. These results indicate that HMGA2 does not randomly recognize any AT-rich sequences. In contrast, it binds to specific AT-rich DNA sequences (21).

Here we decided to study HMGA2-induced DNA conformational change, specifically DNA bending. Since each "AT hook" DNA binding domain contains 5 to 6 positively charges, it should bend the DNA locus upon binding to the AT-rich DNA sequences (22). The challenge is to find a short DNA fragment that does not contain 4 to 5 consecutive AT base pairs for the gel permutation assay. In this case, we can clone one HMGA2 binding site into this short DNA fragment and precisely determine the HMGA2-induced DNA-bending angle without the interference caused by HMGA2 binding to other AT-rich sequences, i.e. sequences containing more than 3 consecutive AT base pairs. In this study, we constructed a new plasmid pBendAT to study HMGA2-induced DNA bending. pBendAT carries a 230 bp DNA sequence that does not contain more that 3 consecutive AT base pairs and therefore does not have an AT-rich sequence. It also contains five pairs of restriction enzyme recognition sites that can be used to generate a set of DNA fragments of identical length to study DNA bending. Using this new plasmid, we demonstrated that HMGA2 bends all three binding sites of HMGA2, SELEX1, SELEX2, and PDRII (the positive regulatory domain II of human interferon-β enhancer (23). HMGA2 was demonstrated to bind to PDRII and increase transcription activities mediate by NF-κB (24)).

Materials and Methods

Protein and synthetic deoxyoligonucleotides

The mammalian high mobility group protein AT-hook 2 (HMGA2) was expressed and purified as described previously (19,25). An extinction coefficient of 5,810 cm^{-1} M^{-1} was used to determine the HMGA2 concentration. Synthetic deoxyoligonucleotides were purchased from MWG-Biotech, Inc. (High Point, NC).

Plasmids

Plasmid pBend2 is a generous gift of S. Adhya (National Institutes of Health). Plasmid pBendAT was constructed by the insertion of a 230 bp PCR product into the EcoRI and HindIII sites of pBend2. The 230 bp PCR product was created in two steps using synthetic deoxyoligonucleotides FL423, FL424, FL425, FL426, FL427, FL428, FL429, and FL430 (Table 1). The first step was to make two 125 bp PCR fragments: one using FL423 and FL424 with 15 bp overlapping DNA sequence as the DNA templates and FL427 and FL428 as the primers; another one using FL425 and FL426 with 15 bp overlapping DNA sequence as the DNA templates and FL429 and FL430 as the primers. The second step was to create the 230 bp PCR fragment using the two 125 bp PCR fragments with 20 bp overlapping DNA sequence as the DNA template and FL427 and FL430 as the primers. The map of pBendAT and the DNA sequence of the 230 bp PCR product are shown in Figure 1. Plasmids pBend2-CRP, pBend2-SELEX1, pBend2-SELEX2, pBend2-PRDII, pBendAT-CRP, pBendAT-SELEX1, pBendAT-SELEX2, and pBendAT-PRDII were created by the insertion of a synthetic XbaI DNA fragment containing a CRP binding site or a HMGA2 binding site into the unique XbaI site of pBend2 or pBendAT, respectively. Table 2 summarizes the main properties of these plasmids. All DNA elements were confirmed by DNA sequencing.

Determination of the protein-induced DNA-bending angle

Plasmids pBendAT derivatives containing a CRP binding site or a HMGA2 binding site (Table 2) were digested by a pair of restriction enzymes BspE1-EagI, KpnI-SphI, NheI-AvrII, BamHI-BglII, and SacI-PstI to produce a set of fragments with identical length and base composition in which the position of the protein-binding site is variable. Alternatively, these DNA fragments were produced using polymerase chain reaction using primers shown in Figure 2. We also used pBend2 derivatives to generate a set of fragments with identical length and base composition in which the position of the protein-binding site is variable after digested with restriction enzymes MluI, NheI, EcoRV, SspI, and BamHI. The DNA fragments were labeled with ^{32}P at 5′ termini by T4 polynucleotide kinase in the presence of γ-^{32}P-ATP. The protein-DNA complexes were formed by addition of 2.0 to 20.0×10^{-9} M of the protein to a solution containing 2×10^{-10} M of ^{32}P-labeled DNA. After equilibration for 60 min at 22 °C, the samples were loaded on a polyacryamide gel to determine the mobility of protein-DNA complexes, which is dependent upon the position of the bound protein, with the lowest mobility present when the protein is bound to the center of the fragment. The bending angle α by which the DNA is bent from linearity was estimated by

$$Cos\left(\frac{\alpha}{2}\right) = \frac{\mu_M}{\mu_E}$$

(1)

where μ_M and μ_E are the mobility of the complex with protein bound at the center and the end of DNA, respectively (26).

Electrophoretic Mobility Shift Assay (EMSA)

DNA fragments containing a DNA-binding site of one DNA-binding protein (the NheI-AvrII fragment of the pBendAT or the EcoRV fragment of pBend2 derivatives) were labeled with ^{32}P at 5′ termini by T4 polynucleotide kinase in the presence of γ-^{32}P-ATP. The protein-DNA complexes were formed by addition of appropriate amounts of the protein to a solution containing 0.2 nM of ^{32}P-labeled DNA in the 1×DNA-binding buffer consisting of 20 mM Tris-HC1 (pH 8.0), 200 mM NaCl, 0.5 mM EDTA, 1 mM DTT, 5 mM MgCl$_2$, and 5% glycerol. After equilibration for 60 min at 22 °C, the samples were loaded on a 8% native polyacryamide gel in 0.5 × TBE buffer (0.045 M Tris-Borate (pH 8.3) and 1 mM EDTA) to separate free and bound DNA. The gels were subsequently dried and visualized by autoradiography or quantified using a Fuji FLA 3000 image analyzer. The radioactivity of the free and bound DNA was determined and used to calculate the binding ratio (R), which is equal to the ratio of the radioactivity of the bound DNA divided by the sum of the radioactivity of the bound and free DNA. The apparent DNA binding constant (K_{app}) was obtained by nonlinear-least-squares fitting the following equation using the program Scientist.

$$R = \frac{(a+x+1/K_{app}) - \sqrt{(a+x+1/K_{app})^2 - 4ax}}{2a}$$

(2)

where *a* and *x* represent the total DNA and the total protein concentration, respectively.

Results and Discussion

Initially, we cloned a few HMGA2 binding sites, such as SELEX1, SELEX2, and PDRII (the positive regulatory domain II of human interferon-β enhancer (23)), into XbaI site of pBend2

to study DNA bending induced by HMGA2. However, we noticed that the 236 bp DNA sequence of pBend2, used to generate a set of circularly permuted fragments, contains multiple AT-rich DNA sequences that may bind to HMGA2 (Figure S1) and therefore interfere with the determination of the DNA-bending angle by HMGA2. Indeed, our gel mobility shift assay confirmed that HMGA2 binds to all these AT-rich DNA sequences (Figure S2). In this case, pBend2 derivatives, i.e. pBend2-SELEX1, pBend2-SELEX2, pBend2-PDRII, cannot be used to precisely determine HMGA2-induced DNA-bending angles. In this study, we decided to construct another pBend plasmid, pBendAT to study HMGA2-induced DNA bending. Our strategy was to create and clone a 230 bp DNA sequence, which does not contain 3 consecutive AT base pairs, into EcoRI and HindIII sites of pBend2 (Figure 1). This 230 bp DNA sequence also contains five pairs of restriction enzyme recognition sites that can be used to generate a set of linear DNA fragments of identical length after cleaved with the pair of restriction enzymes (Figure 2). In addition, this set of the identical-size DNA fragments can be produced using polymerase chain reaction amplification (Figure 2). Since the GC content of these DNA fragments are almost identical (Figure 2), their mobility during electrophoresis is also identical (see below for detail). Figure 1 shows the map of pBendAT and the nt sequence of the 230 bp DNA sequence. Figure 2 shows the set of DNA fragments of identical length that can be generated from pBendAT by restriction digestion or PCR amplification.

Next, we cloned the CRP-binding site of the *lac P1* promoter into the XbaI site of pBendAT to produce plasmid pBendAT-CRP (Table 2) and compared the CRP-induced DNA bending for the DNA fragments generated from plasmids pBend2-CRP and pBendAT-CRP. For pBendAT-CRP, a set of DNA fragments of identical size were also generated by using PCR amplification. Our results are shown in Figure 3. As expected, CRP in the presence of cAMP bends all three sets of DNA fragments. The mobility of CRP-DNA complexes is position-dependent with the highest mobility for CRP bound to either end of the DNA fragments and the lowest mobility for CRP bound to the center of the DNA fragments (Figure 3). The CRP-induced DNA-bending angles were estimated to be ~90° for all three DNA fragments (Table 3), which are consistent with published data (27). We also plotted the relative mobility of the CRP-DNA complexes versus the position of the CRP binding sites of the three DNA fragments, which resulted in the extrapolated bending locus at the center of the CRP-binding site (Figure 3D). These results are also consistent with the published results (27). These studies of CRP-induced DNA bending suggest that pBendAT can be used to study DNA bending induced by sequence-specific DNA-binding proteins.

In order to study HMGA2-induced DNA bending, we cloned three different HMGA2 binding sites, SELEX1, SELEX2 and PDRII into pBendAT to yield pBendAT-SELEX1, pBendAT-SELEX2, and pBendAT-PRDII (Table 2). We determined the binding stoichimtry and the DNA-binding constant of HMGA2 binding to these three DNA-binding sites (the NheI-AvrII fragments of the pBendAT derivatives) using electrophoretic mobility shift assay (EMSA). Our results are shown in Figure 4 and Table 3. In these EMSA experiments, only one shifted band was observed, indicating that the DNA fragments only contains one DNA-binding site for HMGA2 (21). Interestingly, the DNA-binding constants (K) of HMGA2 binding to SELEX1 and SELEX2 were determined to, respectively, be $5.2\pm3.0\times10^7$ and $3.9\pm1.9\times10^7$ M^{-1}, 10-fold higher than K of HMGA2 binding to PRDII ($3.1\pm1.3\times10^6$ M^{-1}). These results suggest that SELEX1 and SELEX2 are indeed the preferred DNA-binding sequences of HMGA2 (21). Our results are summarized in Table 3, which are consistent with the previous published results (21,28). We next determined HMGA2-induced DNA-bending for these DNA-binding sites using the DNA fragments generated from pBendAT-SELEX1, pBendAT-SELEX2, and pBendAT-PRDII by PCR amplification. Our results are shown in Figure 5 and Table 3. The mobility of the five free DNA fragments is identical, indicating no intrinsic curvature for the HMGA2 binding sites, SELEX1, SELEX2, and PRDII. The binding of HMGA2 to these binding sites induces a small bend to all three DNA fragments (Figure 5 and

Table 3). Similar to CRP binding to its binding site, the mobility of HMGA2-DNA complexes is also position-dependent with the highest mobility for HMGA2 bound to either end of the DNA fragments and the lowest mobility for HMGA2 bound to the center of the DNA fragments (Figure 5). The DNA bending angles were calculated to be $34.2\pm2.3°$, $33.5\pm1.7°$, and $35.4\pm1.8°$ for SELEX1, SELEX2, and PRDII, respectively (Table 3). The relative mobility of the HMGA2-DNA complexes was plotted against the position of the HMGA2 binding sites of the three DNA fragments, which resulted in the extrapolated bending locus at the center of the HMGA2-binding site (Figure 5C and 5D). Similar results were also obtained using DNA fragments generated with restriction enzyme digestion (data not shown). Since HMGA contains three AT-hook DNA-binding domains specifically binding to the minor groove of AT-rich DNA sequences, the induced DNA bending may be caused by the neutralization of the negative charges in the minor groove of the two AT-rich sequences in the HMGA2 binding sites (unbalanced interphosphate repulsion (22)). In this case, the HMGA2-induced DNA bend ($\sim35°$) may result from two $17°$ DNA bends that occur in the AT-rich sequences and is toward the minor groove. This analysis is consistent with the phasing analyses published previously (23).

The results presented in this article have great biological implications. The HMGA proteins including HMGA2 are chromatin architectural factors that participate in many nuclear processes, such as transcription regulation, DNA repair, chromatin remodeling, RNA processing, and others (29). The critical role of HMGA proteins is to organize the assembly of the regulatory nucleoprotein complexes for these biological functions. For instance, the first step of the assembly of a functional enhanceosome of the human β-interferon (hINF-β) is to recruit HMGA1a into the two AT rich regions of the hINF-β promoter (two molecules of HMGA1a bind to four sites within the promoter region PRDII and PRDIV (30)). Binding of HMGA1a to the enhancer changes the DNA conformation i.e. DNA bending, allowing cooperative recruitment of other transcription factors such as NF-κB, ATF-2/c-JUN and IRFs that together with HMGA1a, assemble into a highly stable nucleoprotein complex enhanceosome. The enhanceosome then provides a correct surface for other transcription activators cooperating with the RNA polymerase II holoenzyme to initiate transcription (31). It was also demonstrated that HMGA2 binds to the promoter fragment containing the PRDII element and enhances transcriptional activation of hINF-β gene (24,32). HMGA2-induced DNA bending presented in this paper provides a direct evidence for the DNA conformational change of the AT-rich regulatory elements in the enhanceosome upon binding to HMGA proteins.

Conclusion

In this paper, we have constructed a plasmid pBendAT to study DNA bending by the mammalian high mobility group protein AT hook 2 (HMGA2). pBendAT carries a 230 bp DNA fragment that contains 5 pairs of restriction enzyme recognition sites that can be used to generate a set of short DNA fragments of identical size to study protein-induced DNA bending. This set of DNA fragments can also be produced by PRC amplification. Since the 230 bp DNA fragments does not contains 3 consecutive AT base pairs, pBendAT is particularly suitable for the study of DNA-bending induced by the DNA binding proteins recognizing AT-rich DNA sequences. Indeed, using pBendAT, we found that HMGA2 induces a small bend to all three binding sequences, i.e. SELEX1, SELEX2, and PRDII.

Supplementary Material

Refer to Web version on PubMed Central for supplementary material.

Acknowledgments

References

1. Zhou X, Benson KF, Ashar HR, Chada K. Mutation responsible for the mouse pygmy phenotype in the developmentally regulated factor HMGI-C. Nature 1995;376:771–774. [PubMed: 7651535]

2. Anand A, Chada K. In vivo modulation of Hmgic reduces obesity. Nat Genet 2000;24:377–380. [PubMed: 10742101]

3. Reeves R. HMGA proteins: flexibility finds a nuclear niche? Biochem Cell Biol 2003;81:185–195. [PubMed: 12897853]

4. Reeves R, Beckerbauer LM. HMGA proteins as therapeutic drug targets. Prog Cell Cycle Res 2003;5:279–286. [PubMed: 14593722]

5. Klotzbucher M, Wasserfall A, Fuhrmann U. Misexpression of wild-type and truncated isoforms of the high-mobility group I proteins HMGI-C and HMGI(Y) in uterine leiomyomas. Am J Pathol 1999;155:1535–1542. [PubMed: 10550310]

6. Ashar HR, Fejzo MS, Tkachenko A, Zhou X, Fletcher JA, Weremowicz S, Morton CC, Chada K. Disruption of the architectural factor HMGI-C: DNA-binding AT hook motifs fused in lipomas to distinct transcriptional regulatory domains. Cell 1995;82:57–65. [PubMed: 7606786]

7. Schoenmakers EF, Wanschura S, Mols R, Bullerdiek J, Van den BH, Van de Ven WJ. Recurrent rearrangements in the high mobility group protein gene, HMGI- C, in benign mesenchymal tumours. Nat Genet 1995;10:436–444. [PubMed: 7670494]

8. Kazmierczak B, Rosigkeit J, Wanschura S, Meyer-Bolte K, Van de Ven WJ, Kayser K, Krieghoff B, Kastendiek H, Bartnitzke S, Bullerdiek J. HMGI-C rearrangements as the molecular basis for the majority of pulmonary chondroid hamartomas: a survey of 30 tumors. Oncogene 1996;12:515–521. [PubMed: 8637707]

9. Sarhadi VK, Wikman H, Salmenkivi K, Kuosma E, Sioris T, Salo J, Karjalainen A, Knuutila S, Anttila S. Increased expression of high mobility group A proteins in lung cancer. J Pathol 2006;209:206–212. [PubMed: 16521118]

10. Chang ZG, Yang LY, Wang W, Peng JX, Huang GW, Tao YM, Ding X. Determination of high mobility group A1 (HMGA1) expression in hepatocellular carcinoma: a potential prognostic marker. Dig Dis Sci 2005;50:1764–1770. [PubMed: 16187170]

11. Rogalla P, Drechsler K, Schroder-Babo W, Eberhardt K, Bullerdiek J. HMGIC expression patterns in non-small lung cancer and surrounding tissue. Anticancer Res 1998;18:3327–3330. [PubMed: 9858904]

12. Rommel B, Rogalla P, Jox A, Kalle CV, Kazmierczak B, Wolf J, Bullerdiek J. HMGI-C, a member of the high mobility group family of proteins, is expressed in hematopoietic stem cells and in leukemic cells. Leuk Lymphoma 1997;26:603–607. [PubMed: 9389367]

13. Kottickal LV, Sarada B, Ashar H, Chada K, Nagarajan L. Preferential expression of HMGI-C isoforms lacking the acidic carboxy terminal in human leukemia. Biochem Biophys Res Commun 1998;242:452–456. [PubMed: 9446816]

14. Abe N, Watanabe T, Sugiyama M, Uchimura H, Chiappetta G, Fusco A, Atomi Y. Determination of high mobility group I(Y) expression level in colorectal neoplasias: a potential diagnostic marker. Cancer Res 1999;59:1169–1174. [PubMed: 10096541]

15. Meyer B, Loeschke S, Schultze A, Weigel T, Sandkamp M, Goldmann T, Vollmer E, Bullerdiek J. HMGA2 overexpression in non-small cell lung cancer. Mol Carcinog 2007;46:503–511. [PubMed: 17477356]

16. Fusco A, Fedele M. Roles of HMGA proteins in cancer. Nat Rev Cancer 2007;7:899–910. [PubMed: 18004397]

17. Miao Y, Cui T, Leng F, Wilson WD. Inhibition of high-mobility-group A2 protein binding to DNA by netropsin: a biosensor-surface plasmon resonance assay. Anal Biochem 2008;374:7–15. [PubMed: 18023407]

18. Huth JR, Bewley CA, Nissen MS, Evans JN, Reeves R, Gronenborn AM, Clore GM. The solution structure of an HMG-I(Y)-DNA complex defines a new architectural minor groove binding motif. Nat Struct Biol 1997;4:657–665. [PubMed: 9253416]
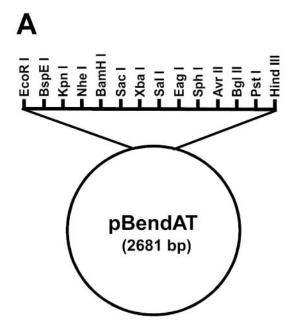
19. Cui T, Wei S, Brew K, Leng F. Energetics of binding the mammalian high mobility group protein HMGA2 to poly(dA-dT)2 and poly(dA)-poly(dT). J Mol Biol 2005;352:629–645. [PubMed: 16109425]

20. Maher JF, Nathans D. Multivalent DNA-binding properties of the HMG-1 proteins. Proc Natl Acad Sci U S A 1996;93:6716–6720. [PubMed: 8692884]

21. Cui T, Leng F. Specific recognition of AT-rich DNA sequences by the mammalian high mobility group protein AT-hook 2: a SELEX study. Biochemistry 2007;46:13059–13066. [PubMed: 17956125]

22. Maher LJ III. Mechanisms of DNA bending. Curr Opin Chem Biol 1998;2:688–694. [PubMed: 9914185]

23. Falvo JV, Thanos D, Maniatis T. Reversal of intrinsic DNA bends in the IFN beta gene enhancer by transcription factors and the architectural protein HMG I(Y). Cell 1995;83:1101–1111. [PubMed: 8548798]

24. Mantovani F, Covaceuszach S, Rustighi A, Sgarra R, Heath C, Goodwin GH, Manfioletti G. NF-kappaB mediated transcriptional activation is enhanced by the architectural factor HMGI-C. Nucleic Acids Res 1998;26:1433–1439. [PubMed: 9490789]

25. Cui T, Joynt S, Morillo V, Baez M, Hua Z, Wang X, Leng F. Large scale preparation of the mammalian high mobility group protein A2 for biophysical studies. Protein Pept Lett 2007;14:87–91. [PubMed: 17266655]

26. Thompson JF, Landy A. Empirical estimation of protein-induced DNA bending angles: applications to lambda site-specific recombination complexes. Nucleic Acids Res 1988;16:9687–9705. [PubMed: 2972993]

27. Kim J, Zwieb C, Wu C, Adhya S. Bending of DNA by gene-regulatory proteins: construction and use of a DNA bending vector. Gene 1989;85:15–23. [PubMed: 2533576]

28. Joynt S, Morillo V, Leng F. Binding the mammalian high mobility group protein AT-hook 2 to AT-rich deoxyoligonucleotides: enthalpy-entropy compensation. Biophys J 2009;96:4144–4152. [PubMed: 19450485]

29. Sgarra R, Zammitti S, Lo SA, Maurizio E, Arnoldo L, Pegoraro S, Giancotti V, Manfioletti G. HMGA molecular network: From transcriptional regulation to chromatin remodeling. Biochim Biophys Acta. 2009

30. Thanos D, Maniatis T. The high mobility group protein HMG I(Y) is required for NF-kappa B-dependent virus induction of the human IFN-beta gene. Cell 1992;71:777–789. [PubMed: 1330326]

31. Thanos D, Maniatis T. Virus induction of human IFN beta gene expression requires the assembly of an enhanceosome. Cell 1995;83:1091–1100. [PubMed: 8548797]

32. Schwanbeck R, Manfioletti G, Wisniewski JR. Architecture of high mobility group protein I-C.DNA complex and its perturbation upon phosphorylation by Cdc2 kinase. J Biol Chem 2000;275:1793–1801. [PubMed: 10636877]

Abbreviations

HMGA2	The mammalian high mobility group protein AT-hook 2
EMSA	Electrophoretic mobility shift assay
nt	nucleotides

A

B

```
EcoRI   BspEI                              KpnI
GAATTCTCCGGACTCGTCGTCCTGGCGGTACCACGCTATC
              NheI                          BamHI
TGTGCAAGGTGCTAGCCACCGGACACGTGCTCCAGGATCC
                            SacI    XbaI   SalI
GAGTGTCCACCACCGAGGTGAAGGAGCTCTCTAGAGTCGA
   EagI                      SphI
CCGGCCGCACCAGGTCAACAGGCATGCACCGGCCTCTTCA
       AvrII                     BglII
TGCGACCTAGGAGCGACCTTCAGCATCGCAGATCTGTCCC
                     PstI      HindIII
TCTGGAGGACGGGAAGTACTGCAGAAGCTT
```

Figure 1.
(A) The map of plasmid pBendAT. (B) The nucleotide sequence of the 230 bp fragment of pBendAT between EcoRI and HindIII sites. The restriction enzyme sites for EcoRI, BspEI, KpnI, NheI, BamHI, SacI, XbaI, SalI, EagI, SphI, AvrII, BglII, PstI, and HindIII are shown.
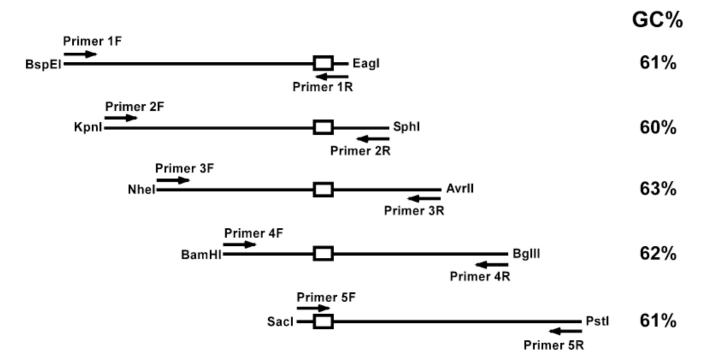
Figure 2.
The five DNA fragments of identical length, which can be produced by restriction enzyme digestion or PCR amplification and used in the DNA-bending experiments, are shown. The GC% is also shown. The open rectangle indicates the DNA-binding site. The following are DNA sequences for the primers: primer 1F, 5′-TCGTCGTCCTGGCGGTAC-3′, 1R, 5′-GCGGCCGGTCGACTCTAG-3′, 2F, 5′-ACCACGCTATCTGTGCAA-3′, 2R, 5′-TGCCTGTTGACCTGGTGC-3′, 3F, 5′-AGCCACCGGACACGTGCT-3′, 3R, 5′-AGGTCGCATGAAGAGGCC-3′, 4F, 5′-TCCGAGTGTCCACCACCG-3′, 4R, 5′-TCTGCGATGCTGAAGGTC-3′, 5F, 5′-ACCGAGGTGAAGGAGCTC-3′, 5R, 5′-TCCAGAGGGACAGATCTG-3′.
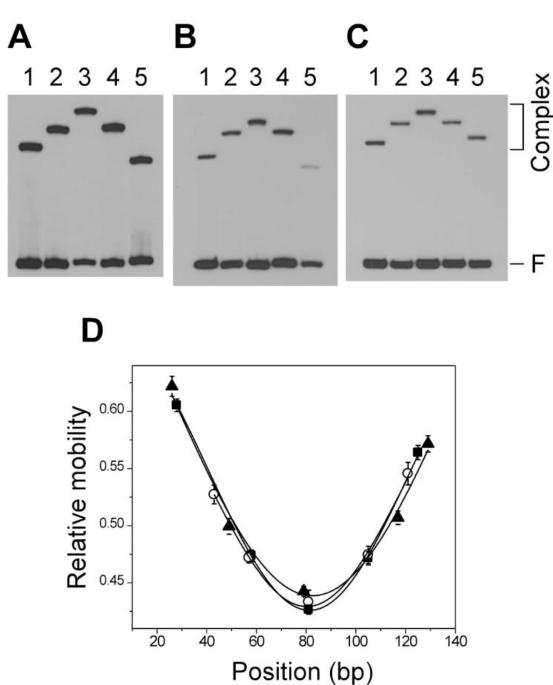
Figure 3.
DNA-bending induced by CRP. DNA-bending assays were carried out as described under Materials and Methods. After the binding of CRP to the permutated DNA fragments in the presence of 20 µM of cAMP, an 8% polyacrylamide gel was used to separate the bound and free DNA fragments. The autoradiograms of ^{32}P-labeled DNA fragments are shown. The DNA fragments in the bottom of the gels are free DNA and those in the upper part are protein-DNA complexes. Labels: F is the free DNA and complex is the protein-DNA complex. (A) The *lac P1* promoter's CRP fragments produced by digestion of plasmid pBend2-CRP with restriction enzymes of MluI, NheI, EcoR V, SspI, and BamHI, respectively. (B) The *lac P1* promoter's CRP fragments produced by digestion of plasmid pBendAT-CRP with a pair of restriction

enzymes of BspEI-EagI, KpnI-SphI, NheI-AvrII, BamHI-BglII, and SacI-PstI, respectively. (C) The *lac P1* promoter's CRP fragments produced using PCR amplification as described in Figure 2. (D) The plot of the relative mobility of CRP-DNA complexes vs. the location of the CRP-binding site within the 159 bp fragment of pBend2 or the 149 bp fragment of pBendAT. Symbols: filled squares, filled triangles, and open circles represent the bending data using the *lac P1* promoter CRP fragments generated by restriction digestion of pBend2-CRP, restriction digestion of pBendAT-CRP, and PCR amplification of pBendAT-CRP, respectively. The standard deviations are also shown.
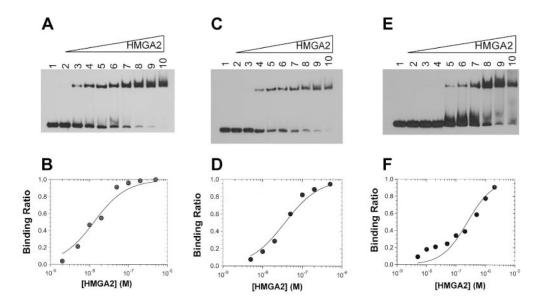
Figure 4.
Quantitative EMSA experiments to determine the DNA-binding constants of HMGA2 binding to SELEX1 (A and B), SELEX2 (C and D), and PRDII (E and F) (the NheI-AvrII fragment of the pBendAT derivatives). 0.2 nM of ³²P-labeled HMGA2 binding fragments were incubated with increasing concentrations of HMGA2 in 50 µl of 1 × EMSA binding buffer containing 20 mM Tris-HCl (pH 8.0), 200 mM NaCl, 0.5 mM EDTA, 1 mM DTT, 0.5 mM MgCl$_2$, and 5 % glycerol. EMSA experiments were performed as described under Materials and Methods. The autoradiograms of the ³²P-labeled FL-SELEX1 are shown. Lane 1 is the free DNA fragment. In addition to the DNA fragment, lanes 2 to 10 also contain 1, 2, 5, 10, 20, 50, 100, 200, and 500 nM of HMGA2, respectively. (B), (D), and (F) are Quantification analysis of the binding data from the EMSA experiments. The bound ratio of DNA was plotted against the protein concentration. The curves are generated from fitting the data to Eq. 2 as described under Materials and Methods.
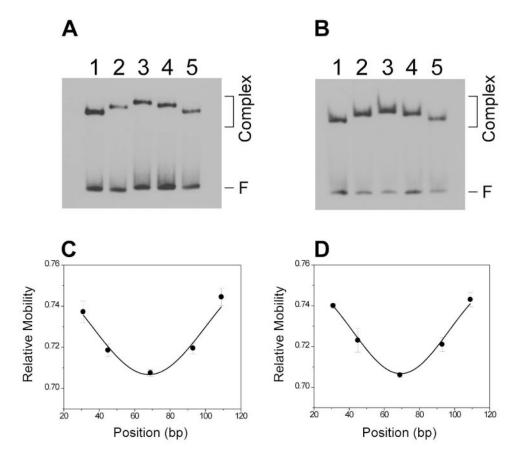
Figure 5.
DNA bending induced by HMGA2. DNA-bending assays were carried out as described under Materials and Methods. After the binding of HMGA2 to the DNA fragments of identical size generated from pBendAT-SELEX1 (A) or pBendAT-SELEX2 (B) by PCR amplification, an 8% polyacrylaimde gel was used to separate the bound and free DNA fragments. The autoradiograms of ^{32}P-labeled DNA fragments are shown. The DNA fragments in the bottom of the gels are free DNA and those in the upper part are protein-DNA complexes. Labels: F is the free DNA and complex is the protein-DNA complex. (C) and (D) are the plots of the relative mobility of HMGA2-DNA complexes vs. the location of the HMGA2-binding site within the 135 bp fragment for pBendAT-SELEX1 or pBendAT-SELEX2, respectively. The standard deviations are also shown.

Table 1

Deoxyoligonucleotides used to construct plasmid pBend-AT

Name	Length (bp)	DNA Sequence
FL423	70	5′-GAATTCTCCGGACTCGTCGTCCTGGCGGTACCACGCTATCTGTGCAAGGTGCTAGCCACCGGACACGTGC-3′
FL424	70	5′-GCCGGTCGACTCTAGAGAGCTCCTTCACCTCGGTGGTGGACACTCGGATCCTGGAGCACGTGTCCGGTGG-3′
FL425	70	5′-GCTCTCTAGAGTCGACCGGCCGCACCAGGTCAACAGGCATGCACCGGCCTCTTCATGCGACCTAGGAGCG-3′
FL426	70	5′-AAGCTTCTGCAGTACTTCCCGTCCTCCAGAGGGACAGATCTGCGATGCTGAAGGTCGCTCCTAGGTCGCA-3′
FL427	21	5′-CCAGAATTCTCCGGACTCGTC-3′
FL428	20	5′-GCCGGTCGACTCTAGAGAGC-3′
FL429	20	5′-GCTCTCTAGAGTCGACCGGC-3′
FL430	22	5′-ACCAAGCTTCTGCAGTACTTCC-3′

Table 2

Plasmids constructed in this study

Plasmid	The DNA-binding site	The DNA binding sequence (top stand)
pBend2-CRP	CRP-binding site	5′-TAATGTGAGTTAGCTCACTCAT-3′
pBendAT-CRP	CRP-binding site	5′-TAATGTGAGTTAGCTCACTCAT-3′
pBend2- SELEX-1	SELEX1	5′-ATATTCGCGATTATT-3′
pBendAT-SELEX-1	SELEX1	5′-ATATTCGCGATTATT-3′
pBend2- SELEX-2	SELEX2	5′-ATATTGCGCATTATT-3′
pBendAT-SELEX-2	SELEX2	5′-ATATTGCGCATTATT-3′
pBend2- PRDII	PRDII	5′-TCGACTGTAAATGACATAGGAAAAC-3′
pBendAT- PRDII	PRDII	5′-TCGACTGTAAATGACATAGGAAAAC-3′

Table 3

The DNA-bending angle and -binding constant of HMGA2 and CRP

The DNA-bind protein	The DNA-binding site	The DNA-binding constant (M^{-1})	The DNA-bending angle (degrees)
CRP	CRP-binding site	$2.8\pm1.1\times10^9$	89.9 ± 0.8[a]
CRP	CRP-binding site	N/A	89.4 ± 1.0[b]
CRP	CRP-binding site	N/A	90.3 ± 0.9[c]
HMGA2	SELEX1	$5.2^d\pm3.0\times10^7$	34.2 ± 2.3[d]
HMGA2	SELEX2	$3.9^d\pm1.9\times10^7$	33.5 ± 1.7[d]
HMGA2	PRDII	$3.1^d\pm1.3\times10^6$	35.4 ± 1.8[d]

[a]CRP-induced DNA bending angle was estimated by using DNA fragments produced by restriction digestion of pBend2-CRP.

[b]CRP-induced DNA bending angle was estimated by using DNA fragments produced by restriction digestion of pBendAT-CRP.

[c]CRP-induced DNA bending angle was estimated by using DNA fragments produced by PCR amplification of pBendAT-CRP.

[d]HMGA2-induced DNA bending angles and the DNA binding constants were determined as described under Materials and Methods. The DNA fragments of identical length were produced by PCR amplification of pBendAT derivatives.